Formation of iron sulfide at faecal pellets and other microniches within sub oxic surface sediment

Anthony Stockdale[*, 1], William Davison, Hao Zhang

Department of Environmental Science, Lancaster Environment Centre (LEC), Lancaster University, Lancaster LA1 4YQ, United Kingdom

[1]**Current address:** Centre for Ecology and Hydrology, Lancaster Environment Centre, Lancaster, LA1 4AP, UK

Published in: Geochimica et Cosmochimica Acta, 2010

The definitive published version is available at: http://dx.doi.org/10.1016/j.gca.2010.02.005

*Corresponding author. Tel +44-1524-595800.
E-mail addresses: tony@biogeochemistry.org.uk (A. Stockdale), w.davison@lancaster.ac.uk (W. Davison), h.zhang@lancaster.ac.uk (H. Zhang).
Fax +44-1524-61536.

Abstract

Faecal pellet deposition and bioturbation may lead to heterogeneously distributed particles of localized highly reactive organic matter (microniches) being present below the oxygen penetration depth. Where O_2, NO_3^-, and Fe/Mn oxyhydroxides become depleted within these microniches or where they exist in zones of sulfate reduction, significant localized peaks in sulfide concentration can occur. These discrete zones of sulfide evolution can cause formation of iron sulfides that would not be predicted by analysis of the 'bulk' sediment. Using a reaction-transport model developed specifically for investigating spherical microniches, and incorporating 3D diffusion, we investigated how the rate constants of organic matter (OM) degradation, particle porosity and niche lifetime, affect dissolved sulfide and iron concentrations, and formation of iron sulfide at such niches. For all of the modelled scenarios the saturation index for iron sulfide is positive, indicating favourable conditions for FeS precipitation in all niches. Those simulations within the microniche lifetime range of 2.5 to 5 days gave comparable concentration ratios of sulfide to iron in solution within the niche to experimentally observed values. Our model results provide insight into the mechanisms of preservation of OM, including soft tissue, in the paleo record, by predicting the conditions that result in preferential deposition of precipitates at the edge of microniches. Decreases in porosity, shorter niche lifetimes and increases in OM degradation rate constants, all tend to increase the likelihood that FeS precipitation will preferentially occur at the edges of a niche, rather than uniformly throughout the niche volume.

1. INTRODUCTION

In stable sediment where oxygen is present at the sediment water interface, bioturbation influences the sediment structure. Due to burrow formation, irrigation, feeding and associated processes, this influence often extends some way into the zone of the sediment usually considered anoxic. These processes create distributions of localized geochemical features associated with active burrows (with surface connection), inactive and infilled burrows, and faecal pellets, and facilitate translocation of surface deposited material, such as marine snow, to greater depths. Here we consider that microniches are formed when discrete particles of reactive organic matter are introduced at depth in the sediment. These microniches can be attributed to decaying organisms (observed using a pH optode; Zhu et al., 2006), algal aggregates (added to sediment to study sulfidic microniches; Widerlund and Davison, 2007) and faecal pellets (photographed after resin embedding and thin sectioning of an intact core; Watling, 1988). The diameter of these microniches can in principle vary from a few microns up to the centimetre scale. However, using high-resolution probes their diameter has generally been observed in the range of 400 µm to ~1 cm (Stockdale et al., 2009; and references therein).

Significant localized peaks in dissolved sulfide (here we use the term sulfide solely to refer to the sum of the dissolved phases H_2S, HS^- and S^{2-}) can occur where microniches become depleted in O_2, NO_3^-, and Fe/Mn oxyhydroxides, or where they exist in zones of sulfate reduction. Localized elevated sulfide formed during the oxidation of microniches of highly reactive organic matter, may provide discrete environments where appreciably more iron sulfide forms than indicated from bulk measurements. With core slicing, for example, there is inherent averaging, and mixing of redox regimes may result in loss of localized sulfides via

oxidation. If locally formed iron sulfides are not subsequently re-oxidized, microniches may account for a significant proportion of FeS or FeS_2 accumulation. Within the upper iron-dominated zone of marine sediments, localized pyrite is commonly associated with microniches of reactive OM (Raiswell, 1993).

Ground breaking diagenetic models, presented by Aller (1980), Berner (1980), Boudreau (1996; and references therein) and van Cappellen and Wang (1996), amongst others, have advanced understanding of sediment systems. With scant information from measurements, understanding of possible processes occurring in microniches has been advanced by modelling. The pioneering study by Jørgensen (1977) investigated the conditions required for a niche to become anoxic within oxic sediment. Raiswell et al. (1993) formulated a basic, 3D, three-component model (Fe^{2+}, sulfide and a pyrite precipitate), relating diffusion and precipitation at the edge of spherical microniches of diameters 50 µm or more. The modelling showed that a greater niche diameter or higher sulfate reduction rate, required increasingly higher dissolved iron concentrations to constrain pyrite precipitation to the niche edge. The diffusion all around niches that is modelled in 3D is not considered in 1D simulations. Multi component modelling in 3D has revealed further complexity in microniche geochemistry. Sochaczewski et al. (2008), showed that within a single microniche near the sediment surface, there can be up to three discrete zones characterised by the dominance of different oxidants (O_2, NO_3^- and SO_4^-). It was assumed that there were no Fe or Mn oxides in the niche. Sulfide is produced because O_2 and NO_3^- are readily consumed in the small volume of the niche.

Here we have modelled, in 3D, the dynamics and spatial distribution of dissolved sulfide, dissolved iron and FeS within and in the vicinity of an idealised spherical particle in suboxic

sediment (below the oxygen and nitrate penetration depths). The modelling was undertaken without use of any fitting parameters so that any correlations to published experimentally observed data are on an a priori basis. The main aim of this study was to examine how ranges of the microniche properties, porosity, OM degradation rate constant and microniche lifetime, affect dissolved sulfide, dissolved iron and FeS concentrations and the nature of FeS precipitation. Further, we will discuss how the results are related to observations and hypotheses from previous studies.

2. MODELLING FRAMEWORK

2.1. Model Description

The sediment model 3D TREAD is a fully three-dimensional diagenetic model specifically designed to investigate processes occurring at spherical microniches. The model, which is applied to a marine sediment here, can be used for either freshwater or marine systems. A brief description of the model is given here; for a more comprehensive account see Sochaczewski et al. (2008).

Rather than providing a rigid framework where components and reactions are fixed, the model lets users specify all required parameters. For each individual component the following conditions can be set: boundary conditions for the top and bottom of the domain (the domain is the modelled volume of sediment, constrained by x, y, and z lengths; the boundary conditions at the sides of the domain are treated as zero flux boundaries); diffusion coefficients; microniche radius, coordinates and concentration; initial profiles (for t = 0 s). Reactions and their rates are then specified for the components of interest. Reactions can be

specified as primary (i.e. organic matter decomposition) or secondary, with primary reactions requiring specification of a priority component (the OM oxidant) and a concentration threshold, below which the reaction with the next priority can begin to proceed. Secondary reactions can be specified as first order for each reactant (overall order based on the number of reactants) or first order for a single component only (overall order of one).

Additional parameters required include: resolution (this controls the density of the 3D mesh), total simulation run time, the time step between each calculation, and the time step between each data save (this allows the output file size to be constrained and reduces output processing times). The vertical porosity profile (and distinct values for each microniche), together with the equation for tortuosity (and associated variables), completes the set-up of the model. As the model inputs are entered via a graphical user interface, parameters can be altered easily, allowing a range of scenarios to be tested.

In adopting a Multi-G approach to organic matter degradation (where different pools of organic matter with different reactivity's are modelled), Westrich and Berner (1984) obtained a ratio of rate constants for the fast reacting pool, $k_{\text{OM-f}}$, to the slow reacting pool, $k_{\text{OM-s}}$, of ~10-17. We have followed, as our starting point, the rates used from the fast and slow reacting pools in Fossing et al. (2002). The ratio of the fast and slow reaction rate constants in this study was 800. Studies of OM mineralization of typical microniche highly reactive material have reported losses of labelled C of 85% over 18 days and 65% over 30 days for carcass and faecal pellets respectively (Lee and Fisher, 1992). For whole phytoplankton debris Newell et al. (1981) measured that over 30% of the OM is mineralized within 3 days, with a more refractory fraction (~64%) taking up to 11 days for mineralization. The ranges of rate constants in this work are consistent with these and other observations of rapid OM

mineralization in the literature (more examples are discussed in section 3.2 in the context of niche lifetimes).

As the effective rate (the rate constant multiplied by the organic matter concentration, adjusted for porosity) of the OM degradation reaction is dependent upon an ever decreasing OM pool the modelled OM concentration will never fall to zero. In defining the lifetime of the niche an arbitrary choice needs to be made. We chose to define the niche lifetime as the time taken for the OM concentration to fall to approximately two thirds of the value at the start of the simulation ($t_{35\%}$).

2.2. Setup of Model Simulations

The reactions applied to the modelling are shown in Table 1 (primary reactions) and Table 2 (secondary reactions). We have excluded phosphorus from the primary reactions in our model, as it takes no part in reactions with the dissolved phases of Fe^{2+} and sulfide. Full model parameters (required inputs as described in section 2.1.) are listed in Table 3. The environmental framework (i.e. the sediment's chemistry and physical properties) is based on a comprehensive data set for a marine sediment by Fossing et al. (2002; 2004). The model reaction and transport equations, and associated parameters in this study, are partly based upon previous studies (Froelich et al., 1979; van Cappellen and Wang, 1996; Wang and van Cappellen, 1996; Rysgaard et al., 1998). These data include all of the required inputs with the exception of the microniche specification. As we model a smaller domain, boundary conditions are derived from the 1D sediment profiles presented by Fossing et al. (2002; 2004). Niches of reactive organic matter are assumed to have negligible iron or manganese oxides available for OM oxidation. Where the niche surface contacts the bulk sediment these

oxidants are assumed to be available. Few data exist on the size distributions and stochastic positions of microniches in sediments. Moreover, these properties are likely to vary greatly depending on the site studied. For these reasons we do not attempt to quantify the total effect of these properties. However, we do discuss what effects microniches may have on overall diagenetic processes and the extent to which bioturbation will negate the influence of iron sulfide formation at microniches.

We have modelled a scenario where the niche is present below the oxygen and nitrate penetration depths (0.67 cm below the sediment water interface), consistent with observed niches in anoxic and suboxic sediments (Widerlund and Davison, 2007; Zhu et al., 2006). This nitrate penetration depth represents the top of the modelled domain and is designated as x = 0 cm in our modelled scenarios. Previous 3D modelling has investigated sulfide evolution in this near surface zone (Sochaczewski et al., 2008). Faecal pellets deposited in situ may typically have nominal diameters of hundreds of µm (e.g. Watling 1988; Wild et al., 2005). However, larger in situ pellets have been observed with nominal diameters of 1.4 to 3.5 mm (Taghon et al., 1984). Nominal diameters of marine snow particles have been observed to cover similar ranges (Alldredge and Cohen, 1987; Shanks and Reeder, 1993), as well as larger values (Hamner et al., 1975). Dead organisms will generally constitute larger microniches than faecal pellets or marine snow. To make this study relevant to each of these particle types we chose a niche diameter of 3 mm.

Several studies have compared the organic matter concentrations in faecal pellets to those from bulk surface sediment (Kristensen and Pilgaard, 2001; Wild et al., 2005). After adjustment for dry weight, the pellets are typically enriched by 11-13 times the OM

concentration in the sediment. We have used a conservative estimate of 5 times the bulk sediment OM in our simulations.

Porosity outside the niche was set as 0.83, consistent with the data compilation used for the 'bulk' values. Microniche porosity was varied to examine its effect. The range considered was from high porosity (φ = 0.97, 0.9) to niches denser (φ = 0.8, 0.7) than the ambient value. Changing porosity has the effect of varying the OM concentration (per unit volume). This gives a maximum range of one order of magnitude to the OM concentration in our simulations. Porosity also has a large affect on the effective diffusion coefficients within microniches. The relationship linking porosity to tortuosity exerts an additional control on the diffusion coefficient calculations. Where niches are more porous than the surrounding sediment, solute transport is faster within the niche. Less porous niches have more restricted transport than in the surrounding sediment. Several studies have investigated the water content and porosity of microniche particles. Plough et al. (2008) measured the porosity of marine snow (φ = 0.996), diatom/phytoplankton aggregates (φ = 0.959-0.992) and faecal pellets of specific organisms (φ = 0.43-0.65). Water content in faecal pellets has been observed to be higher than the ambient sediment (80% compared to 58%; Kristensen and Pilgaard, 2001). The ranges observed in the literature justify our decision to investigate a range of porosities rather than OM concentrations.

2.3. Treatment of Iron-Sulfide Reactions

Sulfide removal mechanisms were via diffusion and reaction with Fe^{2+}. Sulfide formation is solely from the degradation of organic matter with sulfate as the oxidant. S^0 is formed from the oxidation of H_2S by Fe and Mn oxides. Disproportionation of particulate sulfur yields

sulfate and sulfide. Previous modelling by Berg et al., (2003) specifies that the disproportionation reaction to form sulfate and sulfide does not proceed if the sulfide concentration exceeds a critical level of 10 µM. As the sulfide concentration in the modelled microniches rapidly climbs far above the critical level (seconds to minutes), we have excluded this reaction. Iron sulfide precipitation/dissolution reactions are often modelled assuming reversible reactions, typically expressed as separate reactions for formation and dissolution. Whether or not the saturation conditions are met controls which of the two reactions can proceed (see, van Cappellen et al., 1993; Boudreau, 1996; Wang and van Cappellen, 1996; for details of this approach). This relationship is widely used in diagenetic models (Wijsman et al., 2002; Morse and Eldridge, 2007). However, in other modelling cases (e.g. Berg et al., 2002; Fossing et al., 2004) a simple unidirectional formation reaction has been applied (Eq. 1).

$$Fe^{2+} + \sum S(-II) \xrightarrow{k_{FeS}} FeS \qquad (1)$$

A significant advantage of using this approach is that the complexities of modelling pH changes within the model can be avoided. Furthermore, for our modelling this approach is appropriate, as saturation conditions are likely to apply throughout the small domain modelled. Thus the reverse process is negligible and can effectively be excluded.

Several mechanisms have been proposed for the conversion of FeS to pyrite. These include reactions with polysulfide, hydrogen sulfide and reaction pathways with greigite intermediates (Hunger and Benning, 2007 and references therein). There are several approaches to pyrite formation in modelling studies. Berg et al. (2003) and Fossing et al. (2004) modelled formation by reaction of FeS with S^0. Wijsman et al. (2002) used reaction of FeS with H_2S. These two reactions follow the two proposed mechanisms for pyrite formation in nature (Rickard and Morse, 2005). Raiswell (1993) modelled pyrite formation directly

from reaction of Fe(II) and H_2S. Rather than include an additional reaction, Wang and van Cappellen (1996) represented all sulfur-bound iron as FeS. Given the uncertainty regarding the best modelling approach to take, we also represent all sulfur bound iron as FeS. We recognise that these simplifying assumptions limit the degree of detail of the simulations. However, they do not affect the trends in the general features of the solute and solid phase profiles at the microniches.

3. RESULTS AND DISCUSSION

This section reports the results of the modelling and discusses them in terms of:

- trends in iron, sulfide and the related saturation index (SI) with changing porosity, OM degradation rate and niche lifespan.
- relating data from these trends to experimental observations
- assessing the optimum conditions for the formation of FeS crusts at microniches

3.1. Description of Modelled Scenarios

Microniches with various properties were modelled. The effects of porosity and reaction rate of organic matter on the lifespan of a niche are shown to give a general overview, while specific examples considered in more detail examine the generation of sulfide (and associated Fe^{2+}) profiles. The simulation conditions were devised to consider localized sulfide concentrations and the associated 'lifespan' of the niches, while making comparisons with reported reaction rates and experimental observations of niche lifespan. Modelling different porosities allow the results to be interpreted for a range of particle types, from high porosity niches such as algal aggregates to lower porosity particles such as faecal pellets.

3.2. Dissolved Iron(II) and Sulfide at Microniches

3.2.1. Trends Related to Porosity and Rate

Typically observed values for the rate of decomposition of OM, porosity and microniche size were used in the simulations, to ensure that the outputs can be related to realistic environmental scenarios. Figure 1 shows the relationship between reaction rate constants and microniche lifetime for niches with a range of porosities, Table 4 shows the parameters for each of the scenarios in the figure. The lettered data points in Figure 1 represent three groups of data where one of the parameters is constant. Group A (a, b, c, d) has constant porosity, with the decreasing rate constant resulting in an increase in niche lifetime ($t_{35\%}$) across the series. Group B (a, e, f, g) was obtained by setting a series with decreasing porosity and adjusting rate constants to give equal values for $t_{35\%}$ (100 hours). For Group C (g, h, i, d) the rate constant was maintained and $t_{35\%}$ calculated for the range of porosities. Within Group A Multi-G OM mineralization rate constant ratios ($k_{om\text{-}f} : k_{om\text{-}s}$) of 800, 1600, 4000 and 8000 were used to generate outputs for d, c, b and a respectively. The $t_{35\%}$ values for Group B lay within the range of very short microniche lifetimes observed by Alldredge and Cohen (1987) and Zhu et al. (2006). This demonstrates that the use of specific reaction rates for fast reacting organic matter, supports observations of very short niche lifetimes (as discussed in section 2.1.).

Figure 2 shows, for each of the lettered groups and after 2.3 hours of the model simulations, the sulfide and Fe^{2+} concentrations at the centre of the modelled microniches, and the saturation index (SI). The time of 2.3 hours was chosen as this was the maximum time required for the Fe^{2+} and sulfide concentrations to reach a pseudo steady state (i.e. after this

time there were no rapid changes in concentrations of Fe^{2+} and sulfide at the centre of the niche and their concentrations were controlled by removal and resupply processes rather than amounts present at the start of the simulation). Results after 2.3 hours give the maximum sulfide values, as after this time ever decreasing niche OM concentration results in a decreasing sulfide flux. The saturation index (Figure 2) is related to the solubility product of FeS (K_{SP}) and the ion activity products (IAP; Eqs. 2 and 3).

$$IAP = \{Fe^{2+}\}\{HS^-\}/\{H^+\} \quad (2)$$

$$SI = \log(IAP/K_{SP}) \quad (3)$$

IAP was calculated assuming a pH of 7 (consistent with marine porewater values that are typically lower than the overlying water (e.g. Ben-Yaakov, 1973; Zhu et al., 2006) and ionic strength of 0.7 M, with activity coefficients of, γFe^{2+} = 0.255, γHS^- = 0.410, γH^+ = 0.958, (values for Fe^{2+} and H^+ were calculated using the Pitzer equation and associated variables as reported in Millero and Schreiber, 1982; bisulfide value is that reported in Davison, 1980). Decreasing the rate constant and maintaining a fixed porosity (Group A) results in decreasing peak sulfide values, due to lower generation of sulfide fluxes within the niche. The Fe^{2+} concentration at the centre of the niche is determined by several opposing factors. (1) As sulfide produced in the niche diffuses out, it reduces FeOOH in the surrounding sediment and the resulting Fe^{2+} diffuses in. (2) Fe^{2+} is also supplied to the system, as FeOOH is used as an electron acceptor for the oxidation of bulk OM adjacent to the niche. (3) Fe^{2+} is continuously removed at all locations by reaction with HS^- to form FeS. The peaked distribution for Fe^{2+} can be ascribed to changes in the relative dominance of these three processes. The SI is strongly dependent on sulfide for Group A.

Where OM degradation rate constants are adjusted for different porosity microniches, to give equal lifetimes for all niches (Group B), diffusion and reaction with sulfide controls the peak

values of Fe^{2+} and diffusion and the rate constant controls peak sulfide. As the porosity decreases, both diffusion and reaction rates are lowered, decreasing both the inward Fe^{2+} flux and the outward flux of sulfide. In this marine system the sulfate removal rate is not high enough to cause this electron acceptor to become unavailable at the niche centre in any of the modelled scenarios. Limited supply of Fe^{2+} tends to exert the main control on the SI within this group.

Where porosity (φ) is increased at a constant OM degradation rate constant (Group C) sulfide decreases due to a reduced flux caused by the lower physical amount of reactive OM within the niche (accounted for in the model calculation by a (1-φ) function). Across this group the peak concentration of Fe^{2+} increases, as diffusion is faster and removal by sulfide is lower. The highest values for the SI are observed at intermediate porosities. The SI in this group is controlled by more than one species. Within the lowest porosity niche it is constrained by limited diffusion of Fe^{2+} into the niche, while within the highest porosity niche it is constrained by lower sulfide concentrations caused by a reduced sulfide flux. These processes are represented visually in Figure 3, which shows 2D profiles of ∑S(-II), Fe^{2+} and FeS after 24 hours for scenario g. Figure 4 shows a schematic of how FeS may preferentially form at the edges of niche, which is shown by the modelled data in part c of Figure 3.

3.2.2. Relating General Trends from the Modelled Data to Experimental Observations

Peak sulfide concentrations for the microniches are high when compared to porewater values from electrode studies. For example, Sell and Morse (2006) reported a sulfide concentration of ~0.3 μM for a marine sediment, approximately 2 cm below the oxygen penetration depth. If this value is representative of a background measurement, in the modelled microniche, peak concentrations are between ~15 and 240 times the background value. Using DGT to

measure sulfide in a freshwater sediment, Motelica-Heino et al. (2003), reported a sulfidic microniche with concentrations approximately 30 times the average background value, in agreement with the above range. Sagemann et al. (1999) set up laboratory experiments to determine conditions that may result in mineral formation at the soft tissue of benthic organisms (via precipitation of carbonates and phosphates as well as sulfides). They measured sulfide concentrations at the edge of a decomposing shrimp carcass of ~5.6 mM. This value fits into the range of values modelled here (0.46-7.1 mM). These data highlight the stark contrast in the chemistry of microniches compared to their surroundings. Our calculated values for Fe^{2+} concentrations are consistent with observations at similar depths, e.g. Morford et al. (2003) who observed concentrations of ~500 µM at 2 cm depth.

The ratios of the total-sulfide to Fe^{2+} concentrations calculated from the data in Figure 2 fall in the range 1.6 to 169. When the lifetimes greater than 7 days are excluded (Figure 1, points b, c, d and i), the lowest ratio is 30. For microniches within a freshwater lake sediment, sulfide concentrations have been observed to be over 40 times higher than those of Fe^{2+} (Motelica-Heino et al., 2003). These agreements between measurement and modelling further supports the assertion that niche lifetimes of less than one week are the most representative of natural conditions.

3.3. Iron Sulfide at Microniches

The solubility of freshly formed iron sulfide in circumneutral sediment tends to be controlled by the solubility product related to the bisulfide concentration (Eq. 4).

$$FeS_{(s)} + H^+ \underset{}{\overset{K_{FeS}}{\rightleftharpoons}} Fe^{2+} + HS^- \qquad (4)$$

We calculated the distribution of sulfide species in simple sulfide solutions with a pH of 6, 7 and 8, an ionic strength of 0.7 and assuming $[S^{2-}]$ is negligible (activity coefficients were γH^+ = 0.96, γHS^- = 0.41 and γH_2S = 1.0). At pH 6, 7 and 8 approximately 19%, 70% and 96% respectively, of the total sulfide will be present as bisulfide. The pH within marine sediments has been observed to span this range. Zhu et al. (2006), using planar optodes, measured pH at a dead decaying organism (which can be considered a microniche) and reported pH at or below the detection limit of 5.9. Average pH between 1-6 cm below the sediment water interface, in the same sediment without the microniche but with burrowing activity, was ~6.8 with maxima of ~pH 8 and minima of pH $\leq$6.2.

The SI data for Figure 2 were calculated at pH 7. Using these data the degree of saturation of FeS can be calculated. The lowest and highest values for SI are 1.97 and 2.6, equivalent to a degree of saturation of 94 and 400 respectively. It is possible that levels of saturation will not reach these values due to the formation of other mineral phases.

Berner (1980) suggested that concretions of pyrite may be formed by heterogeneous reduction of sulfate at 'clots' of organic matter. The sulfide reacts with Fe^{2+} diffusing towards the niche from the surrounding sediment to form iron sulfides that eventually transform to pyrite. The amount of FeS or pyrite formed is limited by the amount of decomposable organic matter in the niche and the resupply of Fe^{2+}. Berner (1980) proposed that a crust of pyrite will form adjacent to the organic matter. When viewed in 2D as a cross section through the niche, the iron sulfide precipitate appears as a 'halo' shape (Figures 3c and 4). We use the term 'crust' to describe where FeS is preferentially deposited at the edge of the niche rather than continuously throughout the volume. In modelling scenarios a-i in Figure 1, we have determined the distribution of iron sulfide after 24 hours of each of the model runs. Figure 5

shows the vertical FeS profiles through the centre of each niche from these simulations and identifies the profile shape for each of the modelled scenarios. These results show that the only scenario where there is no localisation in FeS formation within the niche has the lowest rate and highest niche lifetime of all the simulations. All other simulations give some localisation within the organic matter parcel. Other simulations with niche lifetimes greater than 145 hours (b, c, i) give localisation within the niche, but do not give significant crustal deposition of FeS. Simulations with short niche lifetimes (<145 hours, a, e, f, g, h) give significant crustal deposition, with ratios of the peak FeS concentration to that at the centre of the niche above 2.7. Within this series, as the porosity and the rate constant decrease the crust becomes more defined. Scenario g (Figure 4) gives the most defined crust with a peak to centre FeS ratio of 7.

The modelling has shown, a priori, that the concept described by Berner (1980) can be explained quantitatively by the microniche model, and that short niche lifetimes give the best results in terms of the definition of the 'crustal' nature of these iron sulfide deposits. In limiting our modelling to FeS, we recognise that preservation of the morphology of the niche will depend on the rate and extent of transformation into pyrite and that this will depend upon the availability of intermediates in the conversion reaction to pyrite (such as polysulfide).

3.3.1. Relevance of Microniche FeS Deposition to Paleoenvironmental Studies

It is important to recognise the significance of the observed precipitation behaviour to the study of the preservation of microniches in the paleo record. Much work has focused on the processes involved in the preservation of 'soft-matter' in the fossil record (e.g. Briggs et al., 1991; 1996; Raiswell et al., 1993; 2008). The conclusion that niche lifetimes of 2.5-5 days give better defined crustal deposition is supported by the work of Sagemann et al. (1999).

They concluded that: 1) mineralization will be dominated by dysaerobic and anaerobic reactions, even in oxic sediments; 2) the most extensive mineral formation of soft tissues occurred under anoxic conditions; 3) steep chemical gradients during the decay process lead to mineral formation; 4) exceptional preservation of soft tissue is favoured by elevated microbial activity; 5) these critical controls that determine the balance between decay and mineral formation (points 1-4) must operate at an early stage following the death of an organism and mineral formation (leading ultimately to fossilisation) of soft tissue must be a rapid process (days to weeks), as it would not occur at the normal 'bulk' efficiency of OM degradation in marine sediments. We have shown that well defined crusts of FeS can occur at microniches in suboxic sediments very rapidly (days). The conditions that favour this formation are where the effective rate (the rate adjusted for the porosity; $k_{OM} \times (1-\varphi)$) gives rapid mineralization of the organic matter. Precipitation at the crust, rather than throughout the volume, is aided by the more restricted diffusion in the lower porosity niches.

Several observations by Briggs et al. (1996), who investigated controls on the pyritization of exceptionally preserved fossils, can be compared to our modelling results. Their work proposed that high dissolved Fe concentrations are the key factor in the preservation of these fossils. Our modelling results indicate that high sulfide concentration can also be a key driver in the formation of a FeS niche with a well preserved structure. However, we recognise that significantly restricted diffusion to/from a niche may also result in well defined localised FeS deposition. Briggs et al. (1996) measured enrichments in $\delta^{34}S$ isotope fractionation within pyritized fossils compared to the surroundings. This enrichment can be explained by either the restricted diffusion or the rapid sulfate consumption hypotheses. Both scenarios will result in restricted supplies of ^{32}S sulfate (that is used preferentially to ^{34}S) to the niche for

OM degradation, and therefore ^{34}S sulfate will be utilised within the niche to a greater degree than the surrounding sediment.

3.4. Other Considerations

3.4.1. Effects of Bioturbation and Bioirrigation.

Exclusion from our model of processes that account for bioirrigation and biodiffusivity, is appropriate given the nature of our modelling. It may be reasonable to expect that in a real system there will be small zones where these processes have no or little effect, at least over time scales of a few days. In our simulations the concentration of Fe^{2+} can build up to levels much higher than would be the case if bioturbation or bioirrigation were included (Figure 3b). The presence of fixed boundaries at the top and bottom of the domain results in an imposed flux out of the domain. In a heterogeneous system with bioturbation, there are likely to be localized zones where solutes diffuse toward secondary interfaces, such as burrows. We accept that our modelled scenarios may be simplistic in the treatment of such behaviour. As bioturbation operates on a larger scale than the microniches, it would be inappropriate to consider its effects as averaged parameters for biodiffusion and bioirrigation. In using diagenetic data from a combined experimental and modelling study (Fossing et al., 2002; 2004), we have excluded any fitting parameters for bioturbation processes so that results reflect only processes occurring at and immediately adjacent to microniches.

Our simulations are performed for a sub-oxic sediment. It may be realistic to suppose that bioturbation may move degraded niches containing FeS to other locations in the sediment, including into the oxic zone. There may be partial or complete removal of localized iron sulfide precipitates due to reoxidation of FeS attributed to bioturbation. The extent of

bioturbation will be important as FeS in undisturbed particles (i.e. remaining present in sub-oxic sediment) is likely to be converted to pyrite, which has slower oxidation rates. Smaller niches relocated to oxic sediment will reoxidize more quickly, so will need to be in contact with oxygenated sediment for shorter times. Certain trace metals sulfides forming at microniches (such as tetrathiomolybdate) may be more resistant to reoxidation (Erickson and Helz, 2000). Therefore, regardless of the degree of bioturbation, microniches may be important zones for the formation of specific trace element sulfides.

3.4.2. Influence of Microniche pH

For simplicity we have assumed a microniche pH of 7 for all calculations in this work. However, complex distributions of pH may occur at microniches. Zhu et al. (2006) observed pH at a dead decaying organism of ≤5.9, where the ambient pH was ~6.6. In this case there is a concentration gradient of protons, which diffuse away from the niche. As pH becomes lower IAP's are reduced by two contributing factors; firstly, the pH term in the denominator of equation 4, and secondly, the equilibrium of sulfide species is shifted towards the H_2S species. The result will be to reduce the formation rate for sulfides at the centre of the niche. As the proton concentration gradient extends from the niche, this effect may enhance FeS formation at the niche edges compared to the niche centre and result in more contrast in the 'halo' effect (i.e. a higher ratio between the FeS at the crust and that in the centre of the niche). This will be the case because the increased proton concentration nearer the centre (compared to the edge) will shift the equilibrium of the FeS formation in the direction of the reverse reaction and thus will bias formation at the niche edge compared to the centre. The lower pH at the niche may be due, in part, to the combined effects of organic matter oxidation (i.e. sulfide formation) and the formation of sulfide phases such as FeS. However, complex buffering processes occur within sediment porewaters (Ben-Yaakov, 1973; Soetaert et al.,

2007). The extent to which the localized geochemistry of a niche allows deviation from buffering effects is a question that requires further study.

3.4.3. Potential Influence of Diffusive Barriers Around Microniches

In the modelling reported here we have assumed that solute transport into and from the niche is controlled exclusively by diffusion (accounting also for the changes to diffusion coefficients induced by porosity changes). Microniches in nature (including faecal pellets and decaying organisms) will have a range of diffusional barriers, which will retard or prevent diffusion across the niche edge. Faecal pellets may possess peritrophic membranes, dead tube dwelling organisms may have a mucus membrane lining the burrow wall at is edge, soft parts of shelled organisms will only have limited exposure to the bulk sediment, and decaying organisms with hard-parts may have complex structures that affect diffusion (see also Stockdale et al., 2009). Where precipitates form surrounding a niche, it is possible that this will create a barrier to diffusion. How diffusive restrictions affect the formation of sulfide precipitates will largely depend upon the resupply of sulfate to the niche interior. In a scenario where diffusion is restricted yet sufficient to resupply sulfate, restriction in the efflux of sulfide will reduce the porewater Fe concentration that is required for precipitation at the niche edge, consistent with the conclusions of Raiswell et al. (1993).

3.4.3. Sensitivity to model assumptions

We have used a conservative estimate for the niche organic matter concentration, of approximately half the value determined by Kristensen and Pilgaard (2001). Whilst the porosity variations modelled here effectively cover a factor of 10 change in the OM concentration, as these changes also affect diffusive transport, it is constructive to test the model for a higher OM concentration at a given porosity. We modelled two niches with the

same parameters as scenarios a and d except the OM concentration was doubled, these scenarios were chosen as they have contrasting niche lifetimes. Increased OM in scenario a resulted in an increase to the definition of the crust (edge to centre FeS ratio of ~8.3, compared to ~2.6 for the lower OM concentration modelling) as well as a higher peak crust FeS concentration. The peak sulfide concentration more than doubles, resulting in a decrease in Fe^{2+}; the IAP is not significantly changed. Increased OM in scenario d approximately doubled the FeS concentration, but did not improve definition of FeS at the crust of the niche.

Whilst many microniche particles will not contain significant levels of Mn or Fe oxides, niches such as faecal pellets from burrowing organisms are likely to contain these oxidants. To test the effect of their presence, we modelled scenario h with the inclusion of oxides at the same level as the surrounding sediment. At the given rate, the Mn and Fe oxides within the niche are exhausted quickly (<3 hrs). This creates a 'pulse' of dissolved Fe that remains elevated for 2-3 hours. After this time (5-6 hrs in total) the profiles show a sulfide peak coincident with Fe^{2+} depletion at the niche centre, similar to scenarios where no oxides are present. Peak FeS levels after 24 hours are elevated by 50% when compared to the same scenario without the oxides present. Preferential deposition at the edge of the niche does not begin to become evident until after 10 hours has elapsed.

4. CONCLUSIONS

We have modelled the behaviour of sulfide and iron within microniches with a range of organic matter (OM) degradation rates and porosities. For all of the modelled scenarios the ion activity product for iron sulfide far exceeds the solubility product, indicating conditions for FeS precipitation in all niches. Those simulations within the $t_{35\%}$ range of 2.5 to 5 days

gave comparable concentration ratios of sulfide to iron in solution within the particles to experimentally observed values. Applying rates for fast reacting OM similar to those in the literature, OM in the niche is rapidly consumed, demonstrating their very short lifetimes.

Our model results provide insight into the mechanisms of preservation of OM, including soft tissue, in the paleo record, by predicting the conditions that result in preferential deposition of precipitates at the edge of microniches. All but one of our simulations showed some localisation of FeS precipitate at the niche. Simulations with short niche lifetimes (<145 hours) give significant crustal deposition, with ratios of the peak FeS concentration to that at the centre of the niche above 2.7. Maximum ratios of crust to centre deposition occur where the niche lifetime is shorter and the porosity is lower. Application of these results to larger scale diagenesis will require a more quantitative assessment of distribution, properties and translocation of microniches within the sediment.

Acknowledgements. AS was supported by the UK Natural Environment Research Council (NER/S/A/2005/13679). We thank Rob Raiswell and John Hamilton-Taylor for constructive comments that led to improvements to an early version of this manuscript. We thank Associate Editor Tim Lyons, Silke Severmann and two anonymous reviewers for thorough reviews that led to significant improvements to the manuscript.

References

Alldredge A.L. and Cohen Y. (1987) Can microscale chemical patches persist in the sea? Microelectrode study of marine snow, fecal pellets. *Science* **235**, 689-691.

Aller R.C. (1980) Quantifying solute distributions in the bioturbated zone of marine sediments by defining an average microenvironment. *Geochim. Cosmochim. Acta* **44**, 1955-1965.

Ben-Yaakov S. (1973) pH buffering of pore water of recent anoxic marine sediments. *Limnol. Oceanogr*. **18**, 86-94.

Berg P., Rysgaard S. and Thamdrup B. (2003) Dynamic modeling of early diagenesis and nutrient cycling. A case study in an arctic marine sediment, *Am. J. Sci.* **303**, 905-955.

Berner R.A., (1980) *Early Diagenesis: A Theoretical Approach*. Princeton University Press, Princeton, pp 241.

Briggs D.E.G., Bottrell S.H. and Raiswell R. (1991) Pyritization of soft-bodied fossils: Beecher's Trilobite Bed, Upper Ordovician, New York State. *Geology* **19**, 1221-1224.

Briggs D.E.G., Raiswell R., Bottrell S.H., Hatfield D. and Bartels C. (1996) Controls on the pyritization of exceptionally preserved fossils: an analysis of the Lower Devonian Hunsrück Slate of Germany. *Am. J. Sci.* **296**, 633-663.

Boudreau B.P. (1996) A method-of-lines code for carbon and nutrient diagenesis. *Comp. Geosci*. **22**, 479-496.

Davison W. (1980) A critical comparison of the measured solubilities of ferrous sulfide in natural waters. *Geochim. Cosmochim. Acta* **44**, 803-808.

Erickson B.E. and Helz G.R. (2000) Molybdenum (VI) speciation in sulfidic waters: stability and lability of thiomolybdates. *Geochim. Cosmochim. Acta* **64**, 1149-1158.

Fossing H., Berg P., Thamdrup B., Rysgaard S., Sørensen H.M. and Nielsen K. (2002) Ilt- og næringsstoffluxmodel for Århus Bugt og Mariager Fjord - *Faglig rapport fra DMU nr. 416*, Danmarks Miljøundersøgelser, pp72.

Fossing H., Berg P., Thamdrup B., Rysgaard S., Sørensen H.M. and Nielsen K. (2004) A model set-up for an oxygen and nutrient flux model for Aarhus Bay (Denmark). *NERI Technical Report No. 483*. National Environmental Research Institute, Denmark, pp65.

Froelich P.N., Klinkhammer G.P., Bender M.L., Luedtke G.R., Heath G.R., Cullen D. and Dauphin P. (1979) Early oxidation of organic matter in pelagic sediments of the eastern equatorial Atlantic: suboxic diagenesis. *Geochim. Cosmochim. Acta* **43**, 1075-1090.

Hamner, W.M., Madin, L.P., Alldrege, A.L., Gilmer, R.W. and Hamner, P.P. (1975) Underwater observations of gelatinous zooplankton: sampling problems, feeding biology, and behavior. *Limnol. Oceanogr*. **20**, 907-917.

Hunger, S., Benning, L.G. (2007) Greigite: a true intermediate on the polysulfide pathway to pyrite. *Geochemical Transactions* **8**:1

Jørgensen B.B. (1977) Bacterial sulfate reduction within reduced microniches of oxidized marine-sediments. *Mar. Biol*. **41**, 7-17.

Kristensen, E. and Pilgaard, R. (2001) The role of fecal pellet deposition by leaf-eating sesarmid crabs on litter decomposition in a mangrove sediment (Phuket, Thailand). In Aller, J.Y., Woodin, S.A. and Aller, R.C., (Eds.), *Organism-Sediment Interactions*, University of South Carolina Press, Columbia, pp. 369-384.

Lee B.-G. and Fisher N.S. (1992) Decomposition and release of elements from zooplankton debris. *Mar. Ecol. Prog. Ser.* **88**, 117-128.

Li, Y.H. and Gregory, S., 1974. Diffusion of ions in sea water and deep sea sediments. *Geochim. Cosmochim. Acta*, **38**, 703-714.

Millero F.J. and Schreiber D.R. (1982) Use of the ion pairing model to estimate activity coefficients of the ionic components of natural waters. *Am. J. Sci*. **282**, 1508-1540.

Morford J., Kalnejais L., Martin W., François R. and Karle I.-M. (2003) Sampling marine pore waters for Mn, Fe, U, Re and Mo: modifications on diffusional equilibration thin film gel probes. *J. Experimental Mar. Biol. Ecol*. **285-286**, 85-103.

Morse J.W. and Eldridge P.M. (2007) A non-steady state diagenetic model for changes in sediment biogeochemistry in response to seasonally hypoxic/anoxic conditions in the "dead zone" of the Louisiana shelf. *Mar. Chem*. **106**, 239-255.

Motelica-Heino M., Naylor C., Zhang H. and Davison W. (2003) Simultaneous release of metals and sulfide in lacustrine sediment. *Environ. Sci. Technol*. **37**, 4374-4381.

Newell R. C., Lucas M. I. and Linley E. A. S. (1981) Rate of degradation and efficiency of conversion of phytoplankton debris by marine micro-organisms. *Mar. Ecol. Prog. Ser*. **6**, 123-136.

Plough H., Iversen M.H. and Fischer G. (2008) Ballast, sinking velocity, and apparent diffusivity within marine snow and zooplankton fecal pellets: Implications for substrate turnover by attached bacteria. *Limnol. Oceanogr*. **53**, 1878-1886.

Raiswell R. (1993) Kinetic controls on depth variations in localised pyrite formation. *Chem. Geol.* **107**, 467-469.

Raiswell R., Whaler K., Dean S., Coleman M.L. and Briggs D.E.G. (1993) A simple three-dimensional model of diffusion-with-precipitation applied to localised pyrite formation in framboids, fossils and detrital iron minerals. *Mar. Geol.* **113**, 89-100.

Raiswell R., Newton R., Bottrell S.H., Coburn P.M., Briggs D.E.G., Bond D.P.G. and Poulton S.W. (2008) Turbidite depositional influences on the diagenesis of Beecher's Trilobite Bed and the Hunsrück Slate; sites of soft tissue pyritization. *Am. J. Sci.* **308**, 105-129.

Rickard D. and Morse J.W. (2005) Acid volatile sulfide (AVS). *Mar. Chem.* **97**, 141–197.

Rysgaard S., Thamdrup B., Risgaard-Petersen N., Fossing H., Berg P., Christensen P.B. and Dalsgaard T. (1998) Seasonal carbon and nitrogen mineralization in a high-Arctic coastal marine sediment, Young Sound, Northeast Greenland. *Mar. Ecol. Prog. Ser*. **179**, 262-276.

Sagemann J., Bale S.J., Briggs D.E.G. and Parkes R.J. (1999) Controls on the formation of authigenic minerals in association with decaying organic matter: an experimental approach. *Geochim. Cosmochim. Acta* **63**, 1083-1095.

Sell K.S. and Morse J.W. (2006) Dissolved Fe^{2+} and $\sum H_2S$ behavior in sediments seasonally overlain by hypoxic-to-anoxic waters as determined by CSV microelectrodes. *Aquatic Geochemistry* **12**, 179–198.

Shanks, A.L. and Reeder, M.L. (1993). Reducing microzones and sulfide production in marine snow. *Mar. Ecol. Prog. Ser.* **96**, 43-47.

Sochaczewski Ł., Stockdale A., Davison W., Tych W. and Zhang H. (2008) A three-dimensional reactive transport model for sediments, incorporating microniches. *Environ. Chem*. **5**, 218-225.

Soetaert K., Hofmann A.F., Middelburg J.J., Meysman F.J.R. and Greenwood J. (2007) The effect of biogeochemical processes on pH. *Mar. Chem.* **105**, 30-51.

Stockdale A., Davison W. and Zhang H. (2009) Micro-scale biogeochemical heterogeneity in sediments: a review of available technology and observed evidence. *Earth-Sci. Rev*. **92**, 81-97.

Taghon G.L., Nowell A.R.M. and Jumars P.A. (1984). Transport and breakdown of fecal pellets: biological and sedimentological consequences. *Limnol. Oceanogr*. **29**, 64-72.

Van Cappellen P. and Wang Y.F. (1996). Cycling of iron and manganese in surface sediments: a general theory for the coupled transport and reaction of carbon, oxygen, nitrogen, sulfur, iron, and manganese. *Am. J. Sci.* 296, 197-243.

Van Cappellen P., Galliard J.-F. and Rabouille C. (1993) Biogeochemical transformations in sediments: kinetic models of early diagenesis. In *Interactions of C, N, P and S Biogeochemical Cycles and Global Change* (eds. R. Woolast, F.T. Mackenzie and L. Chou). Springer-Verlag, Berlin. pp 401-445.

Wang Y. and van Cappellen P. (1996) A multicomponent reactive transport model of early diagenesis: Application to redox cycling in coastal marine sediments. *Geochim. Cosmochim. Acta* **60**, 2993-3014.

Watling L. (1988) Small-scale features of marine sediments and their importance to the study of deposit-feeding. *Mar. Ecol.-Prog. Ser*. **47**, 135-144.

Westrich J.T. and Berner R.A. (1984) The role of sedimentary organic-matter in bacterial sulfate reduction – the G model tested. *Limnol. Oceanogr.* **29**, 236-249.

Widerlund A. and Davison W. (2007) Size and density distribution of sulfide-producing microniches in lake sediments. *Environ. Sci. Technol*. **41**, 8044-8049.

Wijsman J.W.M., Herman P.M.J., Middelburg J.J. and Soetaert K. (2002) A model for early diagenetic processes in sediments of the continental shelf of the Black Sea. *Estuarine Coastal Shelf Sci*. **54**, 403-421.

Wild C., Røy H. and Huettel M. (2005) Role of pelletization in mineralization of fine grained coastal sediments. *Mar. Ecol. Prog. Ser* **291,** 23–33.

Zhu Q.Z., Aller R.C. and Fan Y.Z. (2006) Two-dimensional pH distributions and dynamics in bioturbated marine sediments. *Geochim. Cosmochim. Acta* **70**, 4933-4949.

Tables

Table 1. Primary (organic matter) reactions included in the modelled simulations. H_2O, H^+ and $\sum CO_2$ are included in the reactions for balancing, but are excluded from the model simulations.

$O_2 + OM \xrightarrow{k_{OM}} \sum CO_2 + 0.1NH_4^+ + H_2O$
$0.8NO_3^- + OM + 0.8H^+ \xrightarrow{k_{OM}} \sum CO_2 + 0.1NH_4^+ + 0.4N_2 + 1.4H_2O$
$2MnO_2 + OM + 4H^+ \xrightarrow{k_{OM}} \sum CO_2 + 0.1NH_4^+ + 2Mn^{2+} + 3H_2O$
$4FeOOH + OM + 8H^+ \xrightarrow{k_{OM}} \sum CO_2 + 0.1NH_4^+ + 4Fe^{2+} + 7H_2O$
$0.5SO_4^{2-} + OM + H^+ \xrightarrow{k_{OM}} \sum CO_2 + 0.1NH_4^+ + 0.5\sum H_2S + H_2O$

Table 2. Secondary reactions included in the modelled simulations. H_2O, H^+ and S^0 are included in the reactions for balancing but are excluded from the model simulations.

$NH_4^+ + 2O_2 \xrightarrow{k_6} NO_3^- + H_2O + 2H^+$
$2Mn^{2+} + O_2 + 2H_2O \xrightarrow{k_7} 2MnO_2 + 4H^+$
$4Fe^{2+} + O_2 + 6H_2O \xrightarrow{k_8} 4FeOOH + 8H^+$
$2Fe^{2+} + MnO_2 + 2H_2O \xrightarrow{k_9} 2FeOOH + 2H^+ + Mn^{2+}$
$H_2S + 2FeOOH + 4H^+ \xrightarrow{k_{10}} S^0 + 2Fe^{2+} + 4H_2O$
$H_2S + MnO_2 + 2H^+ \xrightarrow{k_{11}} S^0 + Mn^{2+} + 2H_2O$
$H_2S + Fe^{2+} \xrightarrow{k_{12}} FeS + 2H^+$
$H_2S + 2O_2 \xrightarrow{k_{13}} SO_4^{2-} + 2H^+$
$FeS + 2O_2 \xrightarrow{k_{14}} Fe^{2+} + SO_4^{2-}$

Table 3. Model parameters[a].

Parameter		Value
Domain		x,y,z: 0.7, 0.7, 1.0 cm
Resolution[b]		0.052
Bulk porosity (entered as finite values in the 3d model)		$\varphi = 0.832$
Tortuosity option		Iversen-Jørgensen. n = 2.79
Diffusion coefficients at 10ºC	NH_4^-	13.7×10^{-6} cm^2 s^{-1}
	SO_4^{2-}	7.22×10^{-6} cm^2 s^{-1}
	$\sum H_2S$	11.8×10^{-6} cm^2 s^{-1}
	Mn^{2+}	4.57×10^{-6} cm^2 s^{-1}
	Fe^{2+}	4.48×10^{-6} cm^2 s^{-1}
Boundary conditions[c]		
U = Upper (0.67 cm below SWI)		
L = Lower (1.67 cm below SWI)		
	$[O_2]$	U & L 0 µM
	$[NO_3^-]$	U & L 0 µM
	$[NH_4^-]$	U 36 µM; L 83 µM
	$[Fe^{2+}]$	U 56 µM; L 91 µM
	$[Mn^{2+}]$	U 70 µM; L 60 µM
	$[SO_4^{2-}]$	U & L 20000 µM
	$[\sum H_2S]$	U & L 0 µM
Limiting concentrations (Niche = 2% of bulk value)	$[MnO_2]$	Bulk 1.02×10^5 µM
		Niche 2.04×10^3 µM
	[FeOOH]	Bulk 2.04×10^5 µM
		Niche 4.08×10^3 µM
Rate constants	$k_{OM\text{-}s}$	1.2×10^{-8} s^{-1}
	$k_{OM\text{-}f}$	See Figure 1/Table 4
	k_6	2.5×10^{-6} µM^{-1} s^{-1}
	k_7	1.5×10^{-5} µM^{-1} s^{-1}
	k_8	5.0×10^{-4} µM^{-1} s^{-1}
	k_9	1.7×10^{-8} µM^{-1} s^{-1}
	k_{10}	2.0×10^{-8} µM^{-1} s^{-1}
	k_{11}	3.0×10^{-9} µM^{-1} s^{-1}
	k_{12}	7.5×10^{-7} µM^{-1} s^{-1}
	k_{13}	6.0×10^{-7} µM^{-1} s^{-1}
	k_{14}	5.0×10^{-5} µM^{-1} s^{-1}

All parameters are from Fossing et al. (2002, 2004), except the Fe and Mn diffusion coefficients (Li and Gregory, 1974) and the domain resolution and tortuosity. [b]See Sochaczewski et al. (2008) for a full description of the resolution and mesh density. [c]Boundaries are based on the 1D profiles from Fossing et al. (2002, 2004).

Table 4. Numerical parameters for each of the lettered scenarios in Figure 1.

Scenario	Rate constant (10^{-5} s^{-1})	$t_{35\%}$ (hours)	Porosity (φ)
a	9.60	100	0.97
b	4.80	201	0.97
c	1.92	525	0.97
d	0.96	1000	0.97
e	2.91	100	0.90
f	1.45	100	0.80
g	0.96	100	0.70
h	0.96	145	0.80
i	0.96	302	0.90

Figures

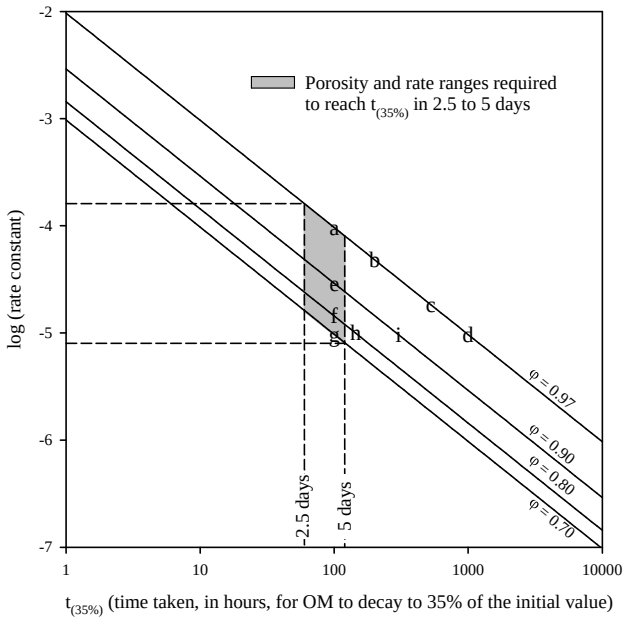

Figure 1. Relationship between the rate constant for the decomposition of organic matter (OM), porosity of the microniche, and the time taken (in hours) for the OM concentration to decay to 35% of the initial value. Letters represent individual data points used in model runs described in the text. Table 4 shows the numerical values for each scenario.

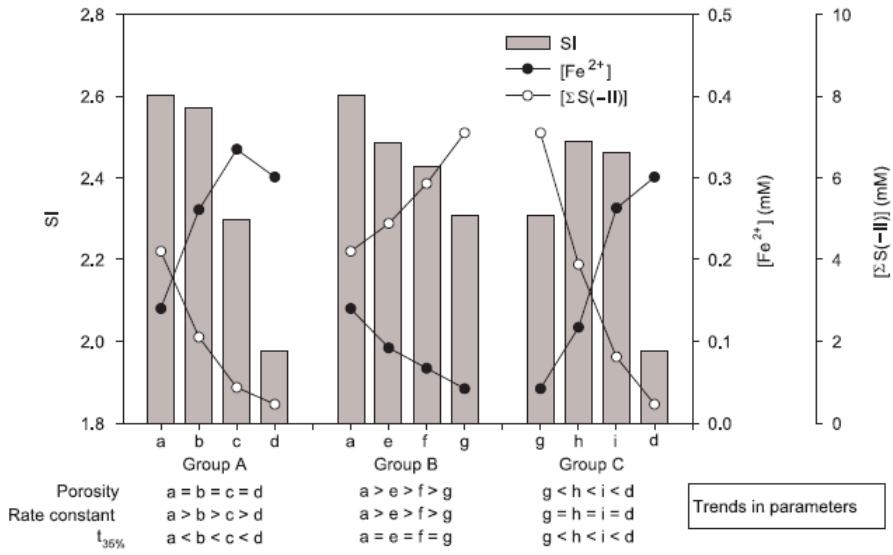

Figure 2. Predicted concentrations of sulfide and Fe^{2+} and the related saturation index (SI) after 2.3 hours of the simulations at the centre of a microniche. The letters represent the data points in Figure 1, where each group of letters has one variable set as a constant. Group A has constant porosity, Group B has conditions where $t_{35\%}$ is constant, Group C has a constant OM degradation rate. Note that the axis for the SI values does not start at zero. The trends relate to the changes associated with the transition across the groups, i.e. a to d, a to g, and g to d.

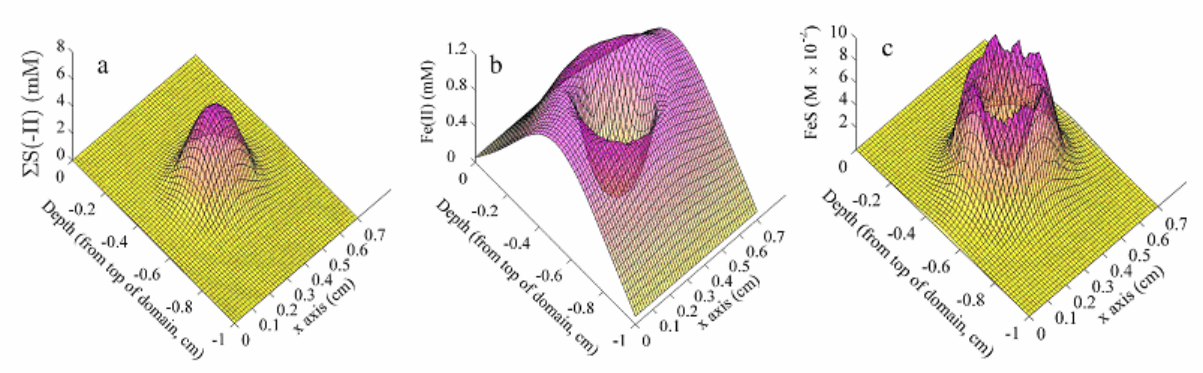

Figure 3. Total sulfide (∑S(-II), a), Fe^{2+} (b) and FeS (c) concentrations across the x axis of the modelled domain after 24 hours (y coordinate was the centre of the microniche). The microniche (scenario g in Figure 1) had a porosity of 0.7, an OM degradation rate constant of 9.6×10^{-6} s^{-1} and an OM concentration of 5 M (representing 21.6 µmol of OM in 14.4 mm^{-3}, volume specific dry mass). The boundary values are explained in section 2.2.

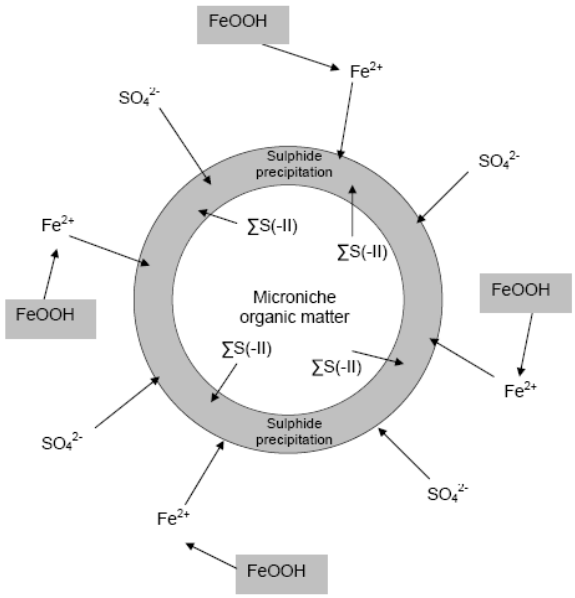

Figure 4. A schematic showing how sulfide precipitation and solute fluxes may occur at a microniche, modified from Berner (1980, p131).

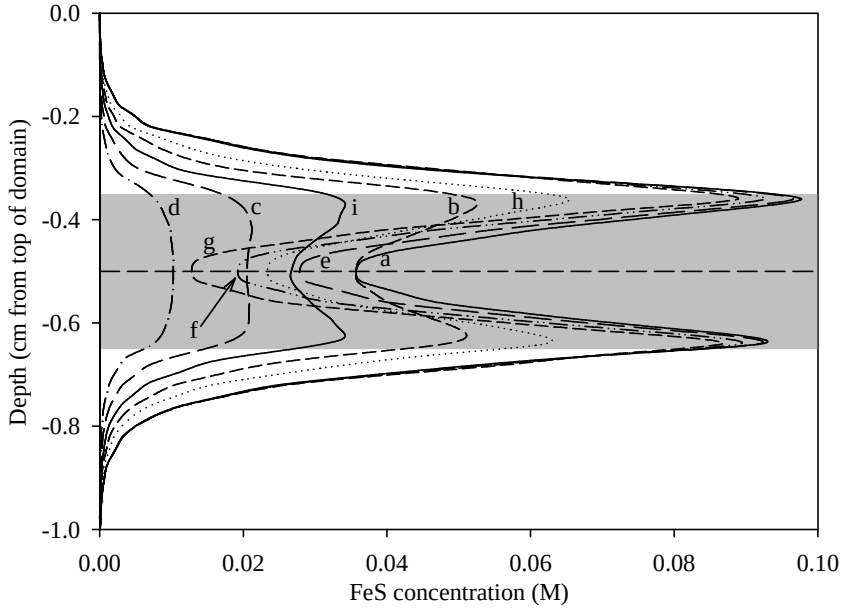

Figure 5. FeS concentrations after a 24 hour model simulation for each of the lettered scenarios in Figure 1. The shaded area represents the locations where the niche is present.